

Geophysical Research Letters[®]



RESEARCH LETTER

10.1029/2022GL102299

Key Points:

- 9 November 2022, earthquake consistent with activity of the Cornelia thrust, a fault system running off the central Adriatic coast
- The seismic reflection profiles in the area allowed for delineating the thrust and its earthquake potential with a much finer resolution
- The properties of the causative fault suggest that the activation of adjacent segments is a plausible scenario that deserves consideration

Supporting Information:

Supporting Information may be found in the online version of this article.

Correspondence to:












F. E. Maesano,
francesco.maesano@ingv.it

Citation:

Maesano, F. E., Buttinelli, M., Maffucci, R., Toscani, G., Basili, R., Bonini, L., et al. (2023). Buried alive: Imaging the 9 November 2022, Mw 5.5 earthquake source on the offshore Adriatic blind thrust front of the Northern Apennines (Italy). *Geophysical Research Letters*, 50, e2022GL102299. <https://doi.org/10.1029/2022GL102299>

Received 29 NOV 2022
Accepted 12 MAY 2023

Buried Alive: Imaging the 9 November 2022, Mw 5.5 Earthquake Source on the Offshore Adriatic Blind Thrust Front of the Northern Apennines (Italy)

F. E. Maesano¹ , M. Buttinelli¹ , R. Maffucci¹, G. Toscani^{2,3} , R. Basili¹ , L. Bonini^{1,4} , P. Burrato¹ , J. Fedorik^{5,6}, U. Fracassi¹ , Y. Panara⁵ , G. Tarabusi¹ , M. M. Tiberti¹ , G. Valensise¹ , R. Vallone¹, and P. Vannoli¹

¹Istituto Nazionale di Geofisica e Vulcanologia, Rome, Italy, ²Dipartimento di Scienze della Terra e dell'Ambiente, Università di Pavia, Pavia, Italy, ³Centro InterUniversitario per l'Analisi SismoTettonica Tridimensionale con Applicazioni Territoriali, Chieti, Italy, ⁴Dipartimento di Matematica e Geoscienze, Università di Trieste, Trieste, Italy, ⁵King Abdullah University of Science and Technology, Thuwal, Saudi Arabia, ⁶Environmental Protection, Saudi Arabian Oil Company, Dhahran, Saudi Arabia

Abstract The prompt identification of faults responsible for moderate-to-large earthquakes is fundamental for understanding the likelihood of further, potentially damaging events. This is increasingly challenging when the activated fault is an offshore buried thrust, where neither coseismic surface ruptures nor GPS/InSAR deformation data are available after an earthquake. We show that on 9 November 2022, an Mw 5.5 earthquake offshore Pesaro ruptured a portion of the buried Northern Apennines thrust front (the Cornelia thrust system [CTS]). By post-processing and interpreting the seismic reflection profiles crossing this thrust system, we determined that the activated fault (CTS) is an arcuate 30-km-long, NW-SE striking, SW dipping thrust and that older structures at its footwall possibly influenced its position and geometry. The activation of adjacent segments of the thrust system is a plausible scenario that deserves to be further investigated to understand the full earthquake potential of this offshore seismogenic source.

Plain Language Summary The Northern Apennines chain is characterized by thrust faults running from the Po Plain to the Adriatic Sea on the northeastern side of peninsular Italy. These thrusts are buried below $\approx 2,000$ m cover of Plio-Pleistocene deposits. Controversies arose about these thrust faults' activity and earthquake potential based on their hidden geological signature and the scanty seismicity that could be associated with them. The earthquake (magnitude 5.5) that occurred on 9 November 2022, offshore Pesaro revived this argument. In this work, we analyze the geological structure of the crustal volume affected by the seismic sequence, exploiting seismic reflection profiles and well-log data to identify the earthquake causative fault. Our results demonstrate that the earthquake ruptured a well-known fault of the Northern Apennines' buried thrust front, supporting that it is indeed active and seismogenic. The size and architecture of this thrust front suggest that it could generate even larger earthquakes ($M_w > 6.5$). This type of geological study is instrumental to understanding the geometry of earthquake faults, particularly in offshore areas, because they constitute reliable inputs for earthquake hazard models and, when done promptly after an earthquake, provide key elements for other studies on the seismic source and the unfolding of the ongoing seismic sequence.

1. Introduction

On 9 November 2022, at 06:07:25 (UTC), an Mw 5.5 earthquake struck offshore Pesaro (central Italy) off the northern Marche coast (Figure 1). Another Ml 5.2 earthquake struck roughly 8 km to the south-southeast 1 min later. The earthquakes referred to as “Costa Marchigiana Pesarese” on the INGV website (<http://terremoti.ingv.it>) were widely felt but caused only minor damage and few secondary environmental effects in the Pesaro-Urbino and Ancona provinces. We refer to this sequence as “Pesaro Offshore.”

The two earthquakes occurred offshore the Northern Apennines contractional belt (NA). The NA developed since the Miocene in various NE-verging arcs, reflecting the paleogeography of the underlying Adria monocline (Amadori et al., 2019; Barchi et al., 1998; Livani et al., 2018; Mariotti & Doglioni, 2000; Mazzoli et al., 2005). The NA outermost thrust likely roots in a common basal detachment (recently modeled by de Nardis et al., 2022) for which geodetic data modeling suggests a present-day active strain consistent with the previous tectonic

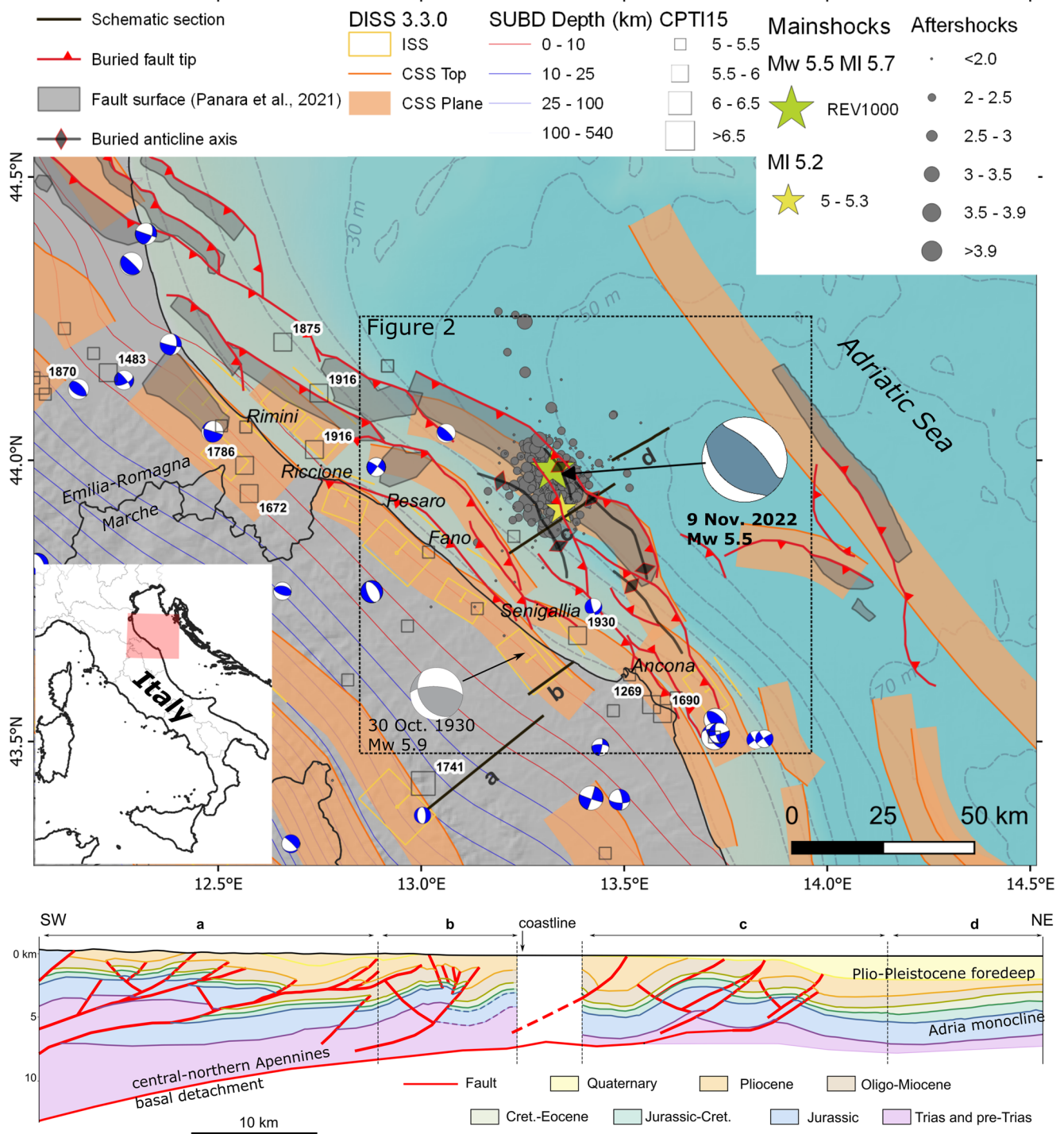


Figure 1. Seismotectonic framework of the northern Adriatic. Mainshock and aftershocks from INGV website and Italian Seismic Bulletin (ISide Working Group, 2007). Focal mechanisms: 2022 eq. and minor seismicity from TDMT (Scognamiglio et al., 2006), 1930 eq. from Vannoli et al., 2015. Historical earthquakes from CPTI15 (Rovida et al., 2022). Seismogenic sources from DISS 3.3.0 (DISS Working Group, 2021); ISS, Individual Seismogenic Source; CSS, Composite Seismogenic Source; Top, upper tip; Plane, surface projection; SUBD Depth, basal detachment depth contours. Fault traces from Bigi et al. (1992), Panara et al. (2021), and Pezzo et al. (2020). The dotted rectangle outlines Figure 2. The bathymetric contours and the Digital Terrain Model are derived from EMODnet Bathymetry Consortium (2020) and SRTM30+ (Becker et al., 2009). Composite schematic section modified from (a) Fantoni and Franciosi (2010), (b) Maesano et al. (2013), (c) Casero and Bigi (2013), and (d) Scrocca et al. (2003).

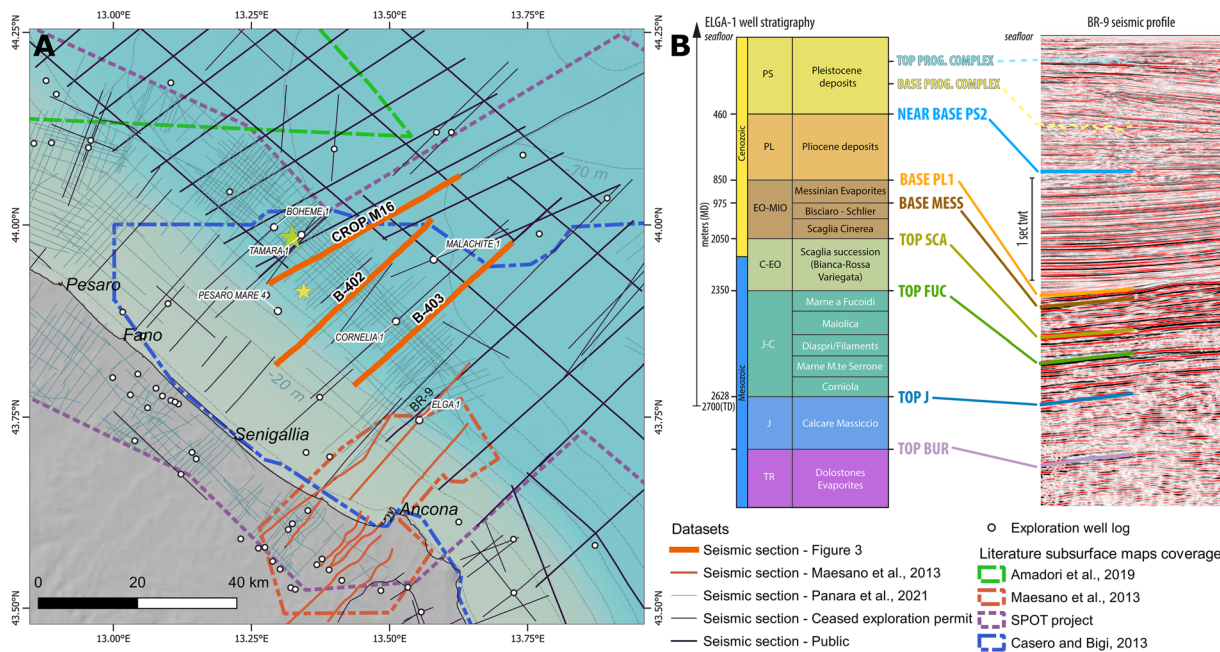


Figure 2. (a) Tracks of seismic reflection profiles, location of well-logs (ViDEPI, CROP), and outline of subsurface maps (Amadori et al., 2019; Antoncicchi et al., 2020; Casero & Bigi, 2013; Maesano et al., 2013; Panara et al., 2021) available for the study area. CROP M16, B-402, and B-403 seismic profiles in Figure 3. (b) Seismostratigraphic scheme derived from Elga-1 well-log, corresponding seismic facies in Table 1.

transport (Carafa et al., 2015; Pezzo et al., 2020). The NA outermost fronts developed during Pliocene and lower Pleistocene times (e.g., Coward et al., 1999; Ghielmi et al., 2013), coalescing into multiple thrusts and associated anticlines (Argnani, 1998; Bigi et al., 1992; Fantoni & Franciosi, 2010; Ghielmi et al., 2010) buried under a thick cover of Plio-Pleistocene marine and continental deposits. Plio-Pleistocene sedimentation rates range from 1 to 2.5 mm/year in the Po Plain (Maesano & D'Ambrogio, 2016) to 1–2 mm/year in the Northern Adriatic Sea (Amadori et al., 2020; Ghielmi et al., 2013). The thrust activity rates decreased since Calabrian times from 1 to 2 mm/year to ca. 0.1 mm/year (Gundersen et al., 2018; Maesano et al., 2015; Panara et al., 2021) and were overtaken by sedimentation rates.

The buried geometry of the NA outer thrusts led to a long-lasting debate concerning its recent and present-day activity. Such questioning rested on the weak geologic-geomorphic deformation signature onshore, the lack of bathymetric signature offshore, and focal mechanisms of small-magnitude earthquakes (Coward et al., 1999; Di Bucci & Mazzoli, 2002; Mazzoli et al., 2015; Troiani & Della Seta, 2011). The recent offshore activity was also attributed to NW-SE transpressional tectonics (Costa et al., 2021; Pierantoni et al., 2019). These conclusions have been highly disputed based on the integration of different observations, including geomorphology, extensive geophysical and subsurface geological datasets, historical seismicity, and focal mechanisms of major earthquakes (Basili & Barba, 2007; Burrato et al., 2003; DISS Working Group, 2021; Maesano et al., 2013; Panara et al., 2021; Vannoli et al., 2004, 2015).

The seismogenic character of the NA buried thrust system became dramatically evident in May 2012, when two earthquakes (Mw 5.9 and Mw 6.1, respectively) occurred within 10 days from one another near Mirandola town, causing 27 casualties and significant damage in a densely populated and heavily industrialized region of the Po Plain (Bonini et al., 2014; Burrato et al., 2012; Nespoli et al., 2018; Pezzo et al., 2013; Scognamiglio et al., 2012; Tertulliani et al., 2012; Tizzani et al., 2013), about 200 km to the NW of Pesaro.

Several Mw ≥ 5.5 earthquakes have struck the northern Marche coastal and offshore area over the past centuries (Table S1 in Supporting Information S1), causing casualties, damage, and seismo-induced environmental effects, including tsunamis (Guidoboni et al., 2018, 2019; Maramai et al., 2021; Rovida et al., 2022), likely generated by seafloor deformation due to dislocation of seismogenic faults at depth (Kastelic et al., 2013; Vannoli et al., 2004, 2015).

Although the elusive nature of buried and blind thrusts hinders their identification and makes it difficult to evaluate their activity, these faults can be the source of significant earthquakes and, if located offshore, tsunamis,

as testified by many cases worldwide (Borrero et al., 2001; Hauksson et al., 1995; Hayes et al., 2010; Lettis et al., 1997; McAuliffe et al., 2015).

In many tectonic contexts, multichannel seismic reflection profiles are one of the most powerful tools to unravel the fault geometries, their associated structures at depth, and their activity rates (e.g., Bergen & Shaw, 2010; Buttinelli et al., 2021; Morley, 2009), and are essential in the case of offshore blind faults (e.g., Rivero & Shaw, 2011).

In this contribution, we show how the analyses and interpretation of publicly available seismic reflection profiles and well-logs allowed us to infer the causative fault of the 9 November 2022 mainshock, since its offshore location makes other direct and indirect methods of investigation inapplicable.

2. Materials and Methods

We integrated published subsurface maps (Amadori et al., 2019; Antoncechi et al., 2020; Casero & Bigi, 2013; Maesano et al., 2013; Panara et al., 2021) with publicly available multichannel seismic profiles from ViDEPI and CROP databases (Figure 2a, <https://www.videpi.com>; <https://www.crop.cnr.it>) to provide a structural description of the rock volume affected by the Pesaro Offshore sequence.

The seismic profiles from the ViDEPI database were converted from raster to SEG-Y format to enhance their integration and interpretation. We adopted the Wiggle2segy code (Sopher, 2018) recently tested and calibrated on this same dataset (Buttinelli et al., 2022). We applied an Automatic Gain Control scaling of the amplitude to improve the signal-to-noise ratio of the SEG-Ys.

We based the seismo-stratigraphic interpretation (Figure 2b) on available well-logs (Boheme-1, Tamara-1, Pesaro Mare-4, Cornelia-1, Elga-1, and Malachite-1); the constraints on the Plio-Pleistocene sequence were adopted from studies in adjacent areas (Amadori et al., 2019, 2020; Ghielmi et al., 2013; Panara et al., 2021). The interpreted seismic profiles were integrated with subsurface maps of the Marne a Fucoidi Fm top horizon (Albian p.p.; Casero & Bigi, 2013) and 3D fault surfaces mapped in the area (Antoncechi et al., 2020; Panara et al., 2021).

We used a multilayer seismic velocity model to depth-convert the seismic reflection profiles. For the Plio-Pleistocene stratigraphy, we relied on an extensive analysis of sonic logs for the central Adriatic (Mancinelli & Scisciani, 2020). This model considers that progressive sediment compaction with depth affects the sandy-marly foredeep sequence, gradually increasing the velocity. For the pre-Pliocene units, we used fixed velocities for each seismo-stratigraphic interval (Table 1) based on the analysis of wells data in adjacent areas (Montone & Mariucci, 2020; Trippetta et al., 2021) and on the sonic log of the Elga-1 well within the study area (Figure 2a).

3. Results

The interpretation of three seismic reflection profiles crossing the Pesaro Offshore earthquake epicentral area, from north to south CROP M16, B-402, and B-403 (Figures 2a and 3; see Figures S1 and S2 in Supporting Information S1 for the uninterpreted version), provided an accurate picture of the geological structures involved in the earthquake sequence.

The eastern part of the CROP M16 profile shows a gentle west-dipping monocline of the Triassic-Miocene succession (Adria monocline), associated with some normal faults within the Mesozoic succession, cutting up to the Miocene with moderate offset (Figure 3a). The Plio-Pleistocene foredeep deposits unconformably cover the Adria monocline with an onlap transgressive contact on the upper-Messinian regional unconformity (Base PL1, Figure 2b).

The Tamara-1 well-log projected onto the western portion of the CROP M16 seismic profile shows the repetition of the Miocene-Pliocene sequences due to the offset of various thrust splays connected at depth on a main ramp (Tamara Thrust System [TTS]). The CROP M16 profile also shows a deeper and less developed thrust below the Tamara-1 well, likely connected to the main ramp (Figure 3 inset A1). The deeper thrust upper tip weakly offsets the Marne a Fucoidi top horizon (Top FUC, Figure 2b) and remains confined within the Mesozoic succession. The reflectors below TTS appear deformed by a velocity pull-up effect caused by the high-velocity carbonates of the hanging wall. Pull-up artifacts are observed in all seismic profiles.

Table 1
Seismostratigraphic Scheme With Seismic Facies and Corresponding Lithostratigraphic Units

Litho unit	Seismic facies	Lithostratigraphic units	Velocity (m/s)
PL-PS	Medium- to high-amplitude, continuous and well-layered seismic reflectors alternated with high amplitude, high frequency reflectors with low-to-middle continuity. Progradational geometries are well imaged in the upper part.	Pliocene deposits mainly represented by clays of deep marine environment, upwardly evolving into shallow water (slope, shelf, and coastal) Pleistocene sequences (sand-rich turbidites and progradational geometries).	$V_0 = 1,849$ $K = 0.5 \text{ Hz}$
EO-MIO	Slightly transparent seismic facies in the lower part. Medium- to high-amplitude strong seismic reflectors in the upper part and heterogeneous seismic pattern, often characterized by strong and discontinuous seismic reflectors. The top is marked by base PL1 seismic reflector imaged by a strong and well-recognizable high-amplitude reflector.	Marly limestones, marls, clayey marls and evaporitic deposits (Scaglia Cinerea, Bisciaro, Schlier Fms. and Messinian evaporites).	$V_i = 3,545$ ± 500
C-EO	Repetition of transparent and medium-to-high amplitude reflectors. The top is marked by top SCA seismic reflector, characterized by generally continuous signals with medium-to-high-amplitude.	Pelagic limestones and marly limestones with chert, locally interbedded with resedimented calcareous-clastic deposits (Scaglia Bianca, Scaglia Rossa, and Scaglia Variegata Fms.).	$V_i = 4,700$ ± 600
J-C	Continuous, medium- to high-amplitude and medium frequency reflectors. The top is marked by top FUC seismic reflector, characterized by strong and continuous signals with high reflection coefficient.	Pelagic limestones, cherty limestones and marls (Corniola, Marne del Monte Serrone, Calcari diasprigni, Calcari e marne a filaments, Maiolica and Marne a Fucoidi Fms.).	$V_i = 5,400$ ± 400
J	Transparent seismic facies embedded between the high amplitude reflectors of Triassic deposits and the layered J-C unit.	Massive or coarsely bedded peritidal limestones (Calcere Massiccio Fm.).	$V_i = 5,900$ ± 500
TR	High-amplitude seismic reflectors, generally layered and continuous. TR reflectors within the unit is generally well recognizable in the entire seismic dataset.	Gypsum-anhydrites and dolostones, with alternating dolostones and packstone-grainstones in the upper part (Dolomia Principale, Anidriti di Burano Fms.).	$V_i = 6,000$ ± 400

Note. The fourth column indicates the velocity values used in the time-to-depth conversion derived from the analyzed well logs (Montone & Mariucci, 2020; Trippetta et al., 2021). V_0 and k are the initial velocity at the top of the PL-PLS unit and the gradient describing the velocity variation with depth, respectively (Mancinelli & Scisciani, 2020); V_i , interval velocity.

The Pesaro Mare-4 well (projected onto the CROP M16, Figure 3a) intercepts the Pleistocene deposits unconformably overlying the Miocene succession. This unconformity is generated by the inner thrust ramp, which controls the uplift of the Mesozoic and Miocene successions. We named this set of faults “Pesaro thrust system” (PTS).

Section B-402 shows two well-developed thrust-related anticlines involving the Mesozoic succession at their cores (Figure 3b). The anticline drilled by the Pesaro Mare-4 well correlates with the western one in the CROP M16 profile, showing a pronounced thickness reduction of the Pliocene deposits in the axial zone, accompanied by a marked unconformity at the base of lower-Pleistocene deposits. The PTS displaces the lower Pleistocene unconformity; its Pleistocene activity also influenced the geometry of the prograding complex bottom and top surfaces (Lower-Middle Pleistocene, Figure 3 inset B1). The Cornelia-1 well penetrates the eastern anticline, highlighting a reverse fault that brings Jurassic dolostones at the hanging wall into contact with lower Cretaceous calcarenites in the footwall. Two thrusts control the anticline (Figure 3, inset B2), the upper acting as the main ramp while the lower splay shows only limited displacement. The Plio-Pleistocene unconformities record the anticline deformation, with an abrupt truncation of the Pliocene reflectors against the Base PS2 unconformity. The latter is tilted eastward, whereas the base and top of the prograding complex recorded only subtle deformation in the anticline forelimb. We interpreted the fault controlling this anticline as correlated with the deeper thrust observed in the CROP M16 profile below the Tamara-1 well and named it the “Cornelia thrust system” (CTS).

Section B-403 is located ~20 km southeast of the mainshock; similarly to B-402, it shows that CTS controls an anticline intercepted by the Cornelia-1 well with an imbricated frontal thrust and a minor backthrust (Figure 3c). In this section, we did not identify the PTS that controls the western anticline in section B-402. Conversely, a minor fault, detached within the Messinian succession in the western part of the profile, may represent the northern closure of the Elga thrust system (ETS) controlling the anticline located to the southeast and drilled by the Elga-1 well. This profile also shows Mesozoic normal faults that displace the Adria monocline and control the transition to the shelf facies of the Adriatic Carbonate Platform (e.g., Casero et al., 1990; Vlahović et al., 2005). The Adriatic Carbonate Platform is recognized in the structural high at the NE end of the section (Figure 3c from

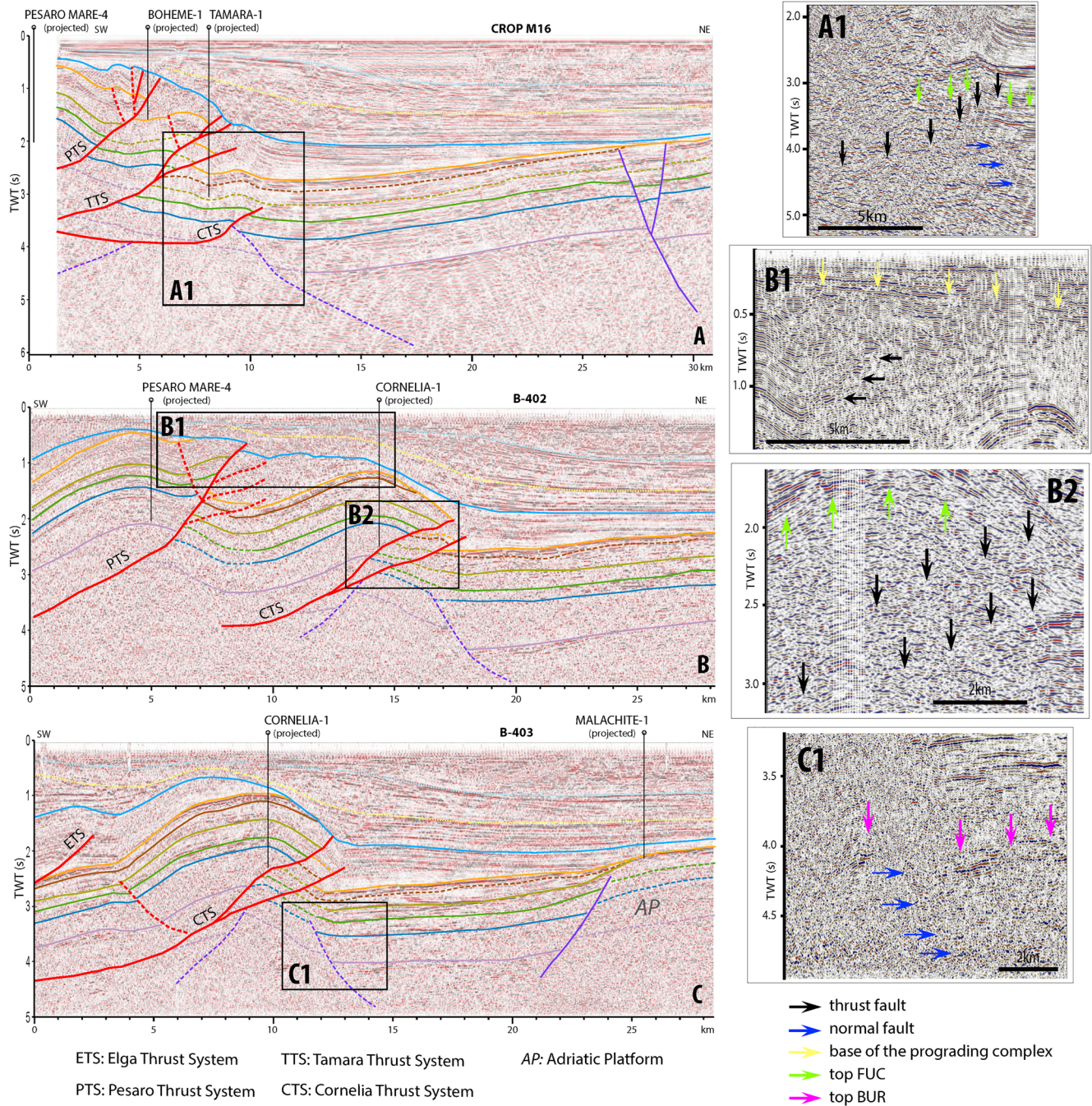


Figure 3. Interpreted seismic reflection profiles (uninterpreted version in Figure S1 in Supporting Information S1; location in Figure 2a). The interpreted top horizons refer to the seismo-stratigraphic scheme of Figure 2b. Insets A1, B1, B2, and C1 show details of the interpretation.

23 to 28 km), where Pliocene deposits unconformably rest upon Eocene successions (in correspondence with Malachite-1 well). The Eocene-Miocene succession is fully preserved in the western-dipping normal fault's hanging wall interpreted in the section's eastern part. In all analyzed seismic profiles it is also possible to tentatively recognize a horst structure in the downgoing Adria monocline at the footwall of the CTS (Figure 3, insets A1 and C1).

Integrating the seismic interpretation with the newly re-interpolated top FUC horizon and fault meshes (Figure 4a) highlights that the outermost Apennines front is characterized by various segments (TTS, CTS, and ETS from north to south). CTS strikes N135 and is at least 28 km long and 10–15 km wide; PTS strikes N150 and is ~25 km

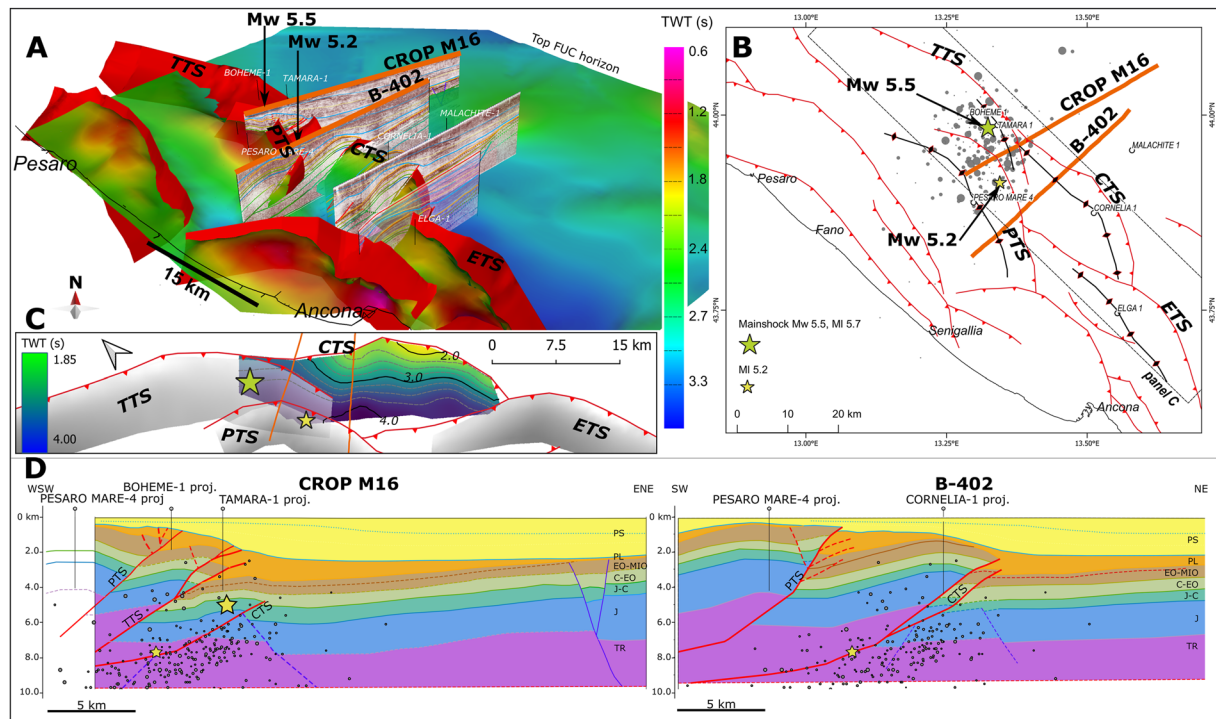


Figure 4. (a) Perspective view of the preliminary 3D tectonic model of the study area. The horizon surface is Top FUC (Figure 2b) modified from Casero and Bigi (2013). Fault surfaces were modified after Casero and Bigi (2013), Maesano et al. (2013), and Panara et al. (2021). (b) Location map of the structural fault model (panel c) and geological sections (panel d). (c) Structural model of the Cornelia thrust system and nearby faults. (d) Geological sections derived from CROP M16 and B-402 profiles (balanced version of B-402 profile in Figure S3 in Supporting Information S1). Mw 5.5 mainshock projected along the strike of the TDMT (128°, Figure 1); aftershocks projected normal-to-section in a buffer of 5 and 10 km for CROP M16 and B-402 profiles, respectively.

long and 10 km wide. The two thrust systems diverge from north to south (Figures 4b and 4c), giving room to a depression bounded by the two anticlines and filled by a Pleistocene prograding complex, deformed by the growing anticlines (B-403 in Figure 3c from 0 to 5 km). The CTS ramp position may be related to a Mesozoic structural high in the footwall of the thrust system (the horst imaged below the Cornelia-1 well, Figure 4d). This structural high bounds a Miocene basin at the CTS footwall (Figure 3c, from 11 to 22 km), confined to the east by west-dipping normal faults, separating it from the Adriatic Carbonate Platform.

To compare the geological reconstruction with the ongoing seismic sequence, we plotted the latest reviewed earthquake locations available from INGV (ISide Working Group, 2007) onto our map and sections. The geological cross-sections derive from the time-to-depth conversion of the seismic profiles (Figure 4d) and were validated through restoration and balancing (Figure S3 in Supporting Information S1). Within the intrinsic uncertainties associated with the network geometry and resolution, the Mw 5.5 mainshock is located ~4 km north of the CROP M16 profile, and its hypocenter lies just 1 km from the CTS, near its upper tip. The MI 5.2 event lies close to the B-402 section and projects at the base of the Cornelia ramp. At the time of writing, the aftershocks of the Pesaro Offshore sequence still affect the area between the CROP M16 and B-402 seismic profiles (Figure 4b). The seismicity projected on these geological cross-sections suggests that most aftershocks concentrate on the CTS (Figure 4d), mimicking its geometry.

4. Discussion and Conclusions

The integration of the geological cross-sections, the distribution of aftershocks, and the re-located mainshock suggests that the Pesaro Offshore sequence occurred on the outermost front of the Northern Apennines (marked as NAF-10 in Panara et al., 2021) and specifically on the buried CTS. This thrust is part of a well-known fault system (Maesano et al., 2013; Panara et al., 2021) already deemed seismogenic (DISS Working Group, 2015).

The mainshock causative fault is characterized by a steep ramp in its central part and becomes more gently dipping toward its northern termination. The structural position of the ramp is possibly controlled by pre-existing

normal faults and associated structural highs in the downgoing Adria monocline (Figure 4c), in agreement with observations in other segments of the NA front (Amadori et al., 2019; Livani et al., 2018).

The mainshock focal mechanisms obtained by various agencies (Table S2 in Supporting Information S1) show an average SW-dipping plane with strike 140°, dip 26°, rake 95°, and a variability of over 20° on each angular estimate. Such values agree very well with the fault geometry and kinematics observed in the geological cross-sections. Due to its offshore setting, the earthquake sequence location may be affected by significant uncertainties arising from the large asymmetry of the recording network and the azimuthal gap. Uncertainties in the horizontal coordinates may vary between 1 and 2 km and can be greater for earthquake depth, which can explain the aftershocks scatter around faults in Figure 4d. Future relocations may reduce uncertainties and allow for further comparison.

The Pesaro Offshore earthquake occurred in a tectonic setting where it is very challenging to identify its causative fault. The moment magnitude implied an earthquake rupture of relatively small size (25–40 km²), according to common scaling relations (Leonard, 2014; Thingbaijam et al., 2017), and remained blind. Also, the hosting fault is part of a larger and articulated offshore fault system. The CTS size (~300 km²) suggests it could host ruptures of up to Mw 6.5 or even larger considering the possible activation with adjacent thrusts. If this were the case, the buried faults of the Adriatic offshore could also generate sizable tsunamis, as observed in the past (Table S1 in Supporting Information S1) and predicted by tsunami scenarios (Antoncecchi et al., 2020; Tiberti et al., 2008). Therefore, this earthquake demonstrated that the CTS is an active and seismogenic fault belonging to a larger fault system extending north and south and toward the Italian coast. Similar faults were previously identified in the area (Argnani, 1998; Bigi et al., 1992; Fantoni & Franciosi, 2010; Maesano et al., 2013; Panara et al., 2021) and should be considered capable of releasing this type of seismicity as already demonstrated by the 1930 Senigallia (Vannoli et al., 2015) and 1987 Porto San Giorgio (Battimelli et al., 2019) earthquakes.

The NA outermost thrusts have generally low activity rates (<1 mm/year during the Pleistocene), and the sedimentation rates in the area are one order of magnitude larger (Maesano et al., 2013, 2015; Maesano & D'Ambrogio, 2016; Panara et al., 2021). Hence, the faults are deeply buried below the Plio-Pleistocene sedimentary succession and, for this reason, were considered inactive (Coward et al., 1999; Di Bucci & Mazzoli, 2002; Mazzoli et al., 2015). Using a constant moment rate approach (Youngs & Coppersmith, 1985), the low slip rates of the NA outermost thrusts imply that larger events have an average recurrence interval of thousands of years. This explains the lack of documented historical earthquakes referable to the CTS. The Pesaro Offshore earthquake demonstrated that the absence of historical and recent seismicity could not exclude the seismogenic potential of active faults, even if they are blind and buried but are geologically documented.

Furthermore, although the Pesaro Offshore earthquake occurred ~30 km offshore, the shaking level onshore (i.e., in the near field) was significant and caused some damage to the built environment (Tertulliani et al., 2022). All these considerations play an important role in devising input data for long-term earthquake hazard models since geological information can provide the accurate location and rupture mechanism of future potential earthquakes. Among the most recent hazard models, such geologic fault information was used to devise earthquake rate forecast input for the new Italian seismic hazard model, MPS19 (Meletti et al., 2021; Visini et al., 2021), the NEAM Tsunami Hazard Model 2018 (Basili et al., 2021), and the European Seismic Hazard Model 2020 (Danciu et al., 2022).

From the short-term perspective, the 3D geometry and structural position of the Pesaro Offshore earthquake causative fault are key elements for studies on the seismic source and the unfolding of the ongoing seismic sequence. The structural interlinkages with adjacent thrusts suggest that activating multiple faults is a plausible scenario that deserves further consideration.

Conflict of Interest

The authors declare no conflicts of interest relevant to this study.

Data Availability Statement

- All data used in this work are publicly accessible. All databases are cited in the relative figure caption and references list.

- Seismic profiles and well-logs are accessible from ViDEPI (<https://www.videpi.com>).
- B-402 <https://www.videpi.com/videpi/sismica/dettaglio.asp?codice=B-402>.
- B-403 <https://www.videpi.com/videpi/sismica/dettaglio.asp?codice=B-403>.
- CROP M16 https://www.videpi.com/deposito/videpi/crop/F_20_M16.pdf.
- CROP M16 SEG-Y can be requested from CNR-ISMAR (www.crop.cnr.it) or consulted at INGV's SismoLab-3D Laboratory (<https://sismolab3d.ingv.it/index.php/en/>).
- CPTI15 <https://doi.org/10.13127/CPTI/CPTI15.4>.
- CFTI5Med <https://doi.org/10.6092/ingv.it-cfti5>.
- ISIDE: <https://webservices.ingv.it/fdsnws/event/1/query?starttime=2022-11-09T00%3A00%3A00&endtime=2022-11-19T23%3A59%3A59&minmag=0&maxmag=10&mindepth=-10&maxdepth=1000&minversion=100&orderby=time-asc&lat=43.8443&lon=13.0206&maxradiuskm=50&format=text&limit=10000>
- TDMT: <http://terremoti.ingv.it/en/event/33301831#MeccanismoFocale>.
- DISS: <https://diss.ingv.it/diss330/sources.php?ITCS106>; <https://doi.org/10.13127/diss3.3.0>.

Acknowledgments

We thank Matteo Basili and two anonymous reviewers for their valuable suggestions. This work was possible thanks to the INGV's Reflection Seismology Laboratory "SismoLab-3D" (<https://sismolab3d.ingv.it/>) infrastructure. Project "Pianeta Dinamico," subtask S2, supported the "SismoLab-3D" for purchasing the CROP data from CNR-ISMAR (<http://crop.cnr.it>). We acknowledge IHS Markit Ltd. for Kingdom Suite Software's educational license and dGB Earth Sciences for the OpendTect software under the General Public License. Earlier interpretations of the datasets are from the SPOT project funded by the Italian Ministry of Economic Development (MISE, DGS-UNMIG) under the umbrella of the offshore safety network "Clypea" and additional resources by projects PRIN 2017 (2017KT2MKE) (P.I.: Giusy Lavecchia; R.U. at University of Pavia; led by Giovanni Toscani) and FASTMIT (Premiale2014 D.M.291 03/05/2016), both funded by the Italian Ministry for University and Research. This work was also supported by the INGV project "Monitoraggio Geotermia Toscana" (Ob. Fu. 1032.010).

References

- Amadori, C., Ghielmi, M., Mancin, N., & Toscani, G. (2020). The evolution of a coastal wedge in response to Plio-Pleistocene climate change: The Northern Adriatic case. *Marine and Petroleum Geology*, *122*, 104675. <https://doi.org/10.1016/j.marpetgeo.2020.104675>
- Amadori, C., Toscani, G., Di Giulio, A., Maesano, F. E., D'Ambrogio, C., Ghielmi, M., & Fantoni, R. (2019). From cylindrical to non-cylindrical foreland basin: Pliocene–Pleistocene evolution of the Po Plain–Northern Adriatic basin (Italy). *Basin Research*, *31*(5), 991–1015. <https://doi.org/10.1111/bre.12369>
- Antonucci, L., Ciccone, F., Dialuce, G., Grandi, S., Terlizze, F., Di Bucci, D., et al. (2020). *Progetto SPOT - Sismicità Potenzialmente Innescaibile Offshore e Tsunami: Report integrato di fine progetto*. 1. Ministero dello Sviluppo Economico. <https://doi.org/10.5281/zenodo.3732887>
- Argnani, A. (1998). Structural elements of the Adriatic foreland and their relationships with the front of the Apennine fold-and-thrust belt. *Memorie della Società Geologica Italiana*, *58*, 647–654.
- Barchi, M. R., DeFeyter, A., Magnani, M. B., Minelli, G., Piali, G., & Sotera, M. (1998). The structural style of the Umbria-Marche fold and thrust belt. *Memorie della Società Geologica Italiana*, *52*, 557–578.
- Basili, R., & Barba, S. (2007). Migration and shortening rates in the northern Apennines, Italy: Implications for seismic hazard. *Terra Nova*, *19*(6), 462–468. <https://doi.org/10.1111/j.1365-3121.2007.00772.x>
- Basili, R., Brizuela, B., Herrero, A., Iqbal, S., Lorito, S., Maesano, F. E., et al. (2021). The making of the NEAM Tsunami Hazard Model 2018 (NEAMTHM18). *Frontiers in Earth Science*, *8*, 616594. <https://doi.org/10.3389/feart.2020.616594>
- Battimelli, E., Adinolfi, G. M., Amoroso, O., & Capuano, P. (2019). Seismic activity in the Central Adriatic offshore of Italy: A review of the 1987 ML 5 Porto San Giorgio earthquake. *Seismological Research Letters*, *90*(5), 1889–1901. <https://doi.org/10.1785/0220190048>
- Becker, J. J., Sandwell, D. T., Smith, W. H. F., Braud, J., Binder, B., Depner, J., et al. (2009). Global bathymetry and elevation data at 30 arc seconds resolution: SRTM30_PLUS. *Marine Geodesy*, *32*(4), 355–371. <https://doi.org/10.1080/01490410903297766>
- Bergen, K. J., & Shaw, J. H. (2010). Displacement profiles and displacement-length scaling relationships of thrust faults constrained by seismic-reflection data. *GSA Bulletin*, *122*(7–8), 1209–1219. <https://doi.org/10.1130/B26373.1>
- Bigi, G., Cosentino, D., Parotto, M., Sartori, R., & Scandone, P. (1992). *Structural model of Italy and gravity map, 1:500,000*. S.E.L.C.A.
- Bonini, L., Toscani, G., & Seno, S. (2014). Three-dimensional segmentation and different rupture behavior during the 2012 Emilia seismic sequence (Northern Italy). *Tectonophysics*, *630*, 33–42. <https://doi.org/10.1016/j.tecto.2014.05.006>
- Borrero, J. C., Dolan, J. F., & Synolakis, C. E. (2001). Tsunamis within the Eastern Santa Barbara Channel. *Geophysical Research Letters*, *28*(4), 643–646. <https://doi.org/10.1029/2000GL011980>
- Burrato, P., Ciucci, F., & Valensise, G. (2003). An inventory of river anomalies in the Po Plain, Northern Italy: Evidence for active blind thrust faulting. *Annals of Geophysics*, *46*(5), 865–882. <https://doi.org/10.4401/ag-3459>
- Burrato, P., Vannoli, P., Fracassi, U., Basili, R., & Valensise, G. (2012). Is blind faulting truly invisible? Tectonic-controlled drainage evolution in the epicentral area of the May 2012, Emilia-Romagna earthquake sequence (northern Italy). *Annals of Geophysics*, *55*(4), 525–531. <https://doi.org/10.4401/ag-6182>
- Buttinelli, M., Maesano, F. E., Sopher, D., Feriozzi, F., Maraio, S., Mazzarini, F., et al. (2022). Revitalizing vintage seismic reflection profiles by converting into SEG-Y format: Case studies from publicly available data on the Italian territory. *Annals of Geophysics*, *65*(5), DM538. <https://doi.org/10.4401/ag-8883>
- Buttinelli, M., Petracchini, L., Maesano, F. E., D'Ambrogio, C., Srococa, D., Marino, M., et al. (2021). The impact of structural complexity, fault segmentation, and reactivation on seismotectonics: Constraints from the upper crust of the 2016–2017 Central Italy seismic sequence area. *Tectonophysics*, *810*, 228861. <https://doi.org/10.1016/j.tecto.2021.228861>
- Carafa, M. M. C., Barba, S., & Bird, P. (2015). Neotectonics and long-term seismicity in Europe and the Mediterranean region. *Journal of Geophysical Research: Solid Earth*, *120*(7), 5311–5342. <https://doi.org/10.1002/2014JB011751>
- Casero, P., & Bigi, S. (2013). Structural setting of the Adriatic basin and the main related petroleum exploration plays. *Marine and Petroleum Geology*, *42*, 135–147. <https://doi.org/10.1016/j.marpetgeo.2012.07.006>
- Casero, P., Rigamonti, A., & Iocca, M. (1990). Paleogeographic relationship during Cretaceous between the Northern Adriatic area and the Eastern Southern Alps. *Memorie della Società Geologica Italiana*, *45*, 807–814.
- Costa, M., Chicco, J., Invernizzi, C., Teloni, S., & Pierantoni, P. P. (2021). Plio–quaternary structural evolution of the outer sector of the Marche Apennines South of the Conero Promontory, Italy. *Geosciences*, *11*(5), 184. <https://doi.org/10.3390/geosciences11050184>
- Coward, M. P., De Donatis, M., Mazzoli, S., Paltrinieri, W., & Wezel, F.-C. (1999). Frontal part of the northern Apennines fold and thrust belt in the Romagna-Marche area (Italy): Shallow and deep structural styles. *Tectonics*, *18*(3), 559–574. <https://doi.org/10.1029/1999TC900003>
- Danciu, L., Weatherill, G., Rovida, A., Basili, R., Bard, P.-Y., Beauval, C., et al. (2022). The 2020 European Seismic Hazard Model: Milestones and lessons learned. In R. Vacareanu & C. Ionescu (Eds.), *Progresses in European earthquake engineering and seismology* (pp. 3–25). Springer International Publishing. https://doi.org/10.1007/978-3-031-15104-0_1

- de Nardis, R., Pandolfi, C., Cattaneo, M., Monachesi, G., Cirillo, D., Ferrarini, F., et al. (2022). Lithospheric double shear zone unveiled by microseismicity in a region of slow deformation. *Scientific Reports*, *12*(1), 21066. <https://doi.org/10.1038/s41598-022-24903-1>
- Di Bucci, D., & Mazzoli, S. (2002). Active tectonics of the Northern Apennines and Adria geodynamics: New data and a discussion. *Journal of Geodynamics*, *34*(5), 687–707. [https://doi.org/10.1016/S0264-3707\(02\)00107-2](https://doi.org/10.1016/S0264-3707(02)00107-2)
- DISS Working Group. (2015). Database of Individual Seismogenic Sources (DISS), version 3.2.0 [Dataset]. Istituto Nazionale di Geofisica e Vulcanologia (INGV). <https://doi.org/10.6092/INGV.IT-DISS3.2.0>
- DISS Working Group. (2021). Database of Individual Seismogenic Sources (DISS), version 3.3.0: A compilation of potential sources for earthquakes larger than M 5.5 in Italy and surrounding areas [Dataset]. Istituto Nazionale Di Geofisica e Vulcanologia (INGV). <https://doi.org/10.13127/DISS3.3.0>
- EMODnet Bathymetry Consortium. (2020). EMODnet Digital Bathymetry (DTM 2020) [Dataset]. EMODnet Bathymetry Consortium. <https://doi.org/10.12770/BB6A87DD-E579-4036-ABE1-E649CEA9881A>
- Fantoni, R., & Franciosi, R. (2010). Tectono-sedimentary setting of the Po Plain and Adriatic foreland. *Rendiconti Lincei*, *21*(1), 197–209. <https://doi.org/10.1007/s12210-010-0102-4>
- Ghielmi, M., Minervini, M., Nini, C., Rogledi, S., & Rossi, M. (2013). Late Miocene–Middle Pleistocene sequences in the Po Plain – Northern Adriatic Sea (Italy): The stratigraphic record of modification phases affecting a complex foreland basin. *Marine and Petroleum Geology*, *42*, 50–81. <https://doi.org/10.1016/j.marpetgeo.2012.11.007>
- Ghielmi, M., Minervini, M., Nini, C., Rogledi, S., Rossi, M., & Vignolo, A. (2010). Sedimentary and tectonic evolution in the eastern Po-Plain and northern Adriatic Sea area from Messinian to Middle Pleistocene (Italy). *Rendiconti Lincei*, *21*(1), 131–166. <https://doi.org/10.1007/s12210-010-0101-5>
- Guidoboni, E., Ferrari, G., Mariotti, D., Comastri, A., Tarabusi, G., Sgattoni, G., & Valensise, G. (2018). CFT15Med, Catalogo dei Forti Terremoti in Italia (461 a.C.-1997) e nell'area Mediterranea (760 a.C.-1500) (Version 5). <https://doi.org/10.6092/INGV.IT-CFT15>
- Guidoboni, E., Ferrari, G., Tarabusi, G., Sgattoni, G., Comastri, A., Mariotti, D., et al. (2019). CFT15Med, the new release of the catalogue of strong earthquakes in Italy and in the Mediterranean area. *Scientific Data*, *6*(1), 80. <https://doi.org/10.1038/s41597-019-0091-9>
- Gunderson, K. L., Anastasio, D. J., Pazzaglia, F. J., & Kodama, K. P. (2018). Intrinsically variable blind thrust faulting. *Tectonics*, *37*(5), 1454–1471. <https://doi.org/10.1029/2017TC004917>
- Hauksson, E., Jones, L. M., & Hutton, K. (1995). The 1994 Northridge earthquake sequence in California: Seismological and tectonic aspects. *Journal of Geophysical Research*, *100*(B7), 12335–12355. <https://doi.org/10.1029/95JB00865>
- Hayes, G. P., Briggs, R. W., Sladen, A., Fielding, E. J., Prentice, C., Hudnut, K., et al. (2010). Complex rupture during the 12 January 2010 Haiti earthquake. *Nature Geoscience*, *3*(11), 800–805. <https://doi.org/10.1038/ngeo977>
- ISIDe Working Group. (2007). Italian Seismological Instrumental and Parametric Database (ISIDe) [Dataset]. <https://doi.org/10.13127/ISIDE>
- Kastelic, V., Vannoli, P., Burrato, P., Fracassi, U., Tiberti, M. M., & Valensise, G. (2013). Seismogenic sources in the Adriatic Domain. *Marine and Petroleum Geology*, *42*, 191–213. <https://doi.org/10.1016/j.marpetgeo.2012.08.002>
- Leonard, M. (2014). Self-consistent earthquake fault-scaling relations: Update and extension to stable continental strike-slip faults. *Bulletin of the Seismological Society of America*, *104*(6), 2953–2965. <https://doi.org/10.1785/0120140087>
- Lettis, W. R., Wells, D. L., & Baldwin, J. N. (1997). Empirical observations regarding reverse earthquakes, blind thrust faults, and quaternary deformation: Are blind thrust faults truly blind? *Bulletin of the Seismological Society of America*, *87*(5), 1171–1198. <https://doi.org/10.1785/bssa0870051171>
- Livani, M., Scrocca, D., Arecco, P., & Doglioni, C. (2018). Structural and stratigraphic control on salient and recess development along a thrust belt front: The Northern Apennines (Po Plain, Italy). *Journal of Geophysical Research: Solid Earth*, *123*(5), 4360–4387. <https://doi.org/10.1002/2017JB015235>
- Maesano, F. E., & D'Ambrogio, C. (2016). Coupling sedimentation and tectonic control: Pleistocene evolution of the central Po Basin. *Italian Journal of Geosciences*, *135*(3), 394–407. <https://doi.org/10.3301/IJG.2015.17>
- Maesano, F. E., D'Ambrogio, C., Burrato, P., & Toscani, G. (2015). Slip-rates of blind thrusts in slow deforming areas: Examples from the Po Plain (Italy). *Tectonophysics*, *643*, 8–25. <https://doi.org/10.1016/j.tecto.2014.12.007>
- Maesano, F. E., Toscani, G., Burrato, P., Mirabella, F., D'Ambrogio, C., & Basili, R. (2013). Deriving thrust fault slip rates from geological modeling: Examples from the Marche coastal and offshore contraction belt, Northern Apennines, Italy. *Marine and Petroleum Geology*, *42*, 122–134. <https://doi.org/10.1016/j.marpetgeo.2012.10.008>
- Mancinelli, P., & Scisciani, V. (2020). Seismic velocity-depth relation in a siliciclastic turbiditic foreland basin: A case study from the Central Adriatic Sea. *Marine and Petroleum Geology*, *120*, 104554. <https://doi.org/10.1016/j.marpetgeo.2020.104554>
- Maramai, A., Graziani, L., & Brizuela, B. (2021). Italian Tsunami Effects Database (ITED): The First database of tsunami effects observed along the Italian coasts. *Frontiers in Earth Science*, *9*, 596044. <https://doi.org/10.3389/feart.2021.596044>
- Mariotti, G., & Doglioni, C. (2000). The dip of the foreland monocline in the Alps and Apennines. *Earth and Planetary Science Letters*, *181*(1), 191–202. [https://doi.org/10.1016/S0012-821X\(00\)00192-8](https://doi.org/10.1016/S0012-821X(00)00192-8)
- Mazzoli, S., Pierantoni, P. P., Borraccini, F., Paltrinieri, W., & Deiana, G. (2005). Geometry, segmentation pattern and displacement variations along a major Apennine thrust zone, central Italy. *Journal of Structural Geology*, *27*(11), 1940–1953. <https://doi.org/10.1016/j.jsg.2005.06.002>
- Mazzoli, S., Santini, S., Macchiavelli, C., & Ascione, A. (2015). Active tectonics of the outer northern Apennines: Adriatic vs. Po Plain seismicity and stress fields. *Journal of Geodynamics*, *84*, 62–76. <https://doi.org/10.1016/j.jog.2014.10.002>
- McAuliffe, L. J., Dolan, J. F., Rhodes, E. J., Hubbard, J., Shaw, J. H., & Pratt, T. L. (2015). Paleoseismologic evidence for large-magnitude (Mw 7.5–8.0) earthquakes on the Ventura blind thrust fault: Implications for multifault ruptures in the Transverse Ranges of southern California. *Geosphere*, *11*(5), 1629–1650. <https://doi.org/10.1130/GES01123.1>
- Meletti, C., Marzocchi, W., D'Amico, V., Lanzano, G., Luzi, L., Martinelli, F., et al. (2021). The new Italian seismic hazard model (MPS19). *Annals of Geophysics*, *64*(1), SE112. <https://doi.org/10.4401/ag-8579>
- Montone, P., & Mariucci, M. T. (2020). Constraints on the structure of the shallow crust in Central Italy from geophysical log data. *Scientific Reports*, *10*(1), 3834. <https://doi.org/10.1038/s41598-020-60855-0>
- Morley, C. (2009). Geometry of an oblique thrust fault zone in a deepwater fold belt from 3D seismic data. *Journal of Structural Geology*, *31*(12), 1540–1555. <https://doi.org/10.1016/j.jsg.2009.08.015>
- Nespoli, M., Belardinelli, M. E., Gualandi, A., Serpelloni, E., & Bonafede, M. (2018). Poroelasticity and fluid flow modeling for the 2012 Emilia-Romagna earthquakes: Hints from GPS and InSAR data. *Geofluids*, *2018*, 1–15. <https://doi.org/10.1155/2018/4160570>
- Panara, Y., Maesano, F. E., Amadori, C., Fedorik, J., Toscani, G., & Basili, R. (2021). Probabilistic assessment of slip rates and their variability over time of offshore buried thrusts: A case study in the Northern Adriatic Sea. *Frontiers in Earth Science*, *9*, 664288. <https://doi.org/10.3389/feart.2021.664288>

- Pezzo, G., Boncori, J. P. M., Tolomei, C., Salvi, S., Atzori, S., Antonioli, A., et al. (2013). Coseismic deformation and source modeling of the May 2012 Emilia (Northern Italy) earthquakes. *Seismological Research Letters*, 84(4), 645–655. <https://doi.org/10.1785/0220120171>
- Pezzo, G., Petracchini, L., Devoti, R., Maffucci, R., Anderlini, L., Antonceccchi, I., et al. (2020). Active fold-thrust belt to foreland transition in Northern Adria, Italy, tracked by seismic reflection profiles and GPS offshore data. *Tectonics*, 39(11), e2020TC006425. <https://doi.org/10.1029/2020TC006425>
- Pierantoni, P. P., Chicco, J., Costa, M., & Invernizzi, C. (2019). Plio-Quaternary transpressive tectonics: A key factor in the structural evolution of the outer Apennine–Adriatic system, Italy. *Journal of the Geological Society*, 176(6), 1273–1283. <https://doi.org/10.1144/jgs2018-199>
- Rivero, C., & Shaw, J. H. (2011). Active folding and blind thrust faulting induced by basin inversion processes, inner California borderlands. In K. McClay, J. Shaw, & J. Suppe (Eds.), *Thrust fault-related folding*. American Association of Petroleum Geologists. <https://doi.org/10.1306/13251338M943432>
- Rovida, A., Locati, M., Camassi, R., Lolli, B., Gasperini, P., & Antonucci, A. (2022). Catalogo Parametrico dei Terremoti Italiani (CPTI15), versione 4.0 [Dataset]. Istituto Nazionale di Geofisica e Vulcanologia (INGV). <https://doi.org/10.13127/CPTI/CPTI15.4>
- Scognamiglio, L., Margheriti, L., Mele, F. M., Tinti, E., Bono, A., De Gori, P., et al. (2012). The 2012 Pianura Padana Emiliana seismic sequence: Locations, moment tensors and magnitudes. *Annals of Geophysics*, 55(4), 5. <https://doi.org/10.4401/ag-6159>
- Scognamiglio, L., Tinti, E., & Quintiliani, M. (2006). Time Domain Moment Tensor (TDMT) [Dataset]. Istituto Nazionale di Geofisica e Vulcanologia (INGV). <https://doi.org/10.13127/TDMT>
- Scrocca, D., Doglioni, C., Innocenti, F., Manetti, P., Mazzotti, A., Bertelli, L., et al. (2003). CROP ATLAS-seismic reflection profiles of the Italian crust. In *Memorie descrittive della Carta geologica d'Italia* (Vol. 62, p. 193).
- Sopher, D. (2018). Converting scanned images of seismic reflection data into SEG-Y format. *Earth Science Informatics*, 11(2), 241–255. <https://doi.org/10.1007/s12145-017-0329-z>
- Tertulliani, A., Antonucci, A., Berardi, M., Borghi, A., Brunelli, G., Caracciolo, C. H., et al. (2022). Gruppo Operativo Quest Rilievo Macro-sismico Mw 5.5 Costa Marchigiana Del 9/11/2022 Rapporto Finale Del 15/11/2022 (Report). Retrieved from <https://www.earth-prints.org/handle/2122/15794>
- Tertulliani, A., Arcoraci, L., Berardi, M., Bernardini, F., Brizuela, B., Castellano, C., et al. (2012). The Emilia 2012 sequence: A macroseismic survey. *Annals of Geophysics*, 55(4), 21. <https://doi.org/10.4401/ag-6140>
- Thingbaijam, K. K. S., Martin Mai, P., & Goda, K. (2017). New empirical earthquake source-scaling laws. *Bulletin of the Seismological Society of America*, 107(5), 2225–2246. <https://doi.org/10.1785/0120170017>
- Tiberti, M. M., Lorito, S., Basili, R., Kastelic, V., Piatanesi, A., & Valensise, G. (2008). Scenarios of earthquake-generated tsunamis for the Italian Coast of the Adriatic Sea. *Pure and Applied Geophysics*, 165(11), 2117–2142. <https://doi.org/10.1007/s00024-008-0417-6>
- Tizzani, P., Castaldo, R., Solaro, G., Pepe, S., Bonano, M., Casu, F., et al. (2013). New insights into the 2012 Emilia (Italy) seismic sequence through advanced numerical modeling of ground deformation InSAR measurements: Modeling of 2012 Emilia Seismic Sequence. *Geophysical Research Letters*, 40(10), 1971–1977. <https://doi.org/10.1002/grl.50290>
- Trippetta, F., Barchi, M. R., Tinti, E., Volpe, G., Rosset, G., & De Paola, N. (2021). Lithological and stress anisotropy control large-scale seismic velocity variations in tight carbonates. *Scientific Reports*, 11(1), 9472. <https://doi.org/10.1038/s41598-021-89019-4>
- Troiani, F., & Della Seta, M. (2011). Geomorphological response of fluvial and coastal terraces to Quaternary tectonics and climate as revealed by geostatistical topographic analysis: Geostatistical topographic analysis of fluvial and coastal terraces. *Earth Surface Processes and Landforms*, 36(9), 1193–1208. <https://doi.org/10.1002/esp.2145>
- Vannoli, P., Basili, R., & Valensise, G. (2004). New geomorphic evidence for anticlinal growth driven by blind-thrust faulting along the northern Marche coastal belt (central Italy). *Journal of Seismology*, 8(3), 297–312. <https://doi.org/10.1023/B:JOSE.0000038456.00574.e3>
- Vannoli, P., Vannucci, G., Bernardi, F., Palombo, B., & Ferrari, G. (2015). The source of the 30 October 1930 Mw 5.8 Senigallia (Central Italy) earthquake: A convergent solution from instrumental, macroseismic, and geological data. *Bulletin of the Seismological Society of America*, 105(3), 1548–1561. <https://doi.org/10.1785/0120140263>
- Visini, F., Pace, B., Meletti, C., Marzocchi, W., Akinci, A., Azzaro, R., et al. (2021). Earthquake rupture forecasts for the mps19 seismic hazard model of Italy. *Annals of Geophysics*, 64(2), SE220. <https://doi.org/10.4401/ag-8608>
- Vlahović, I., Tišljarić, J., Velić, I., & Matičec, D. (2005). Evolution of the Adriatic Carbonate Platform: Palaeogeography, main events and depositional dynamics. *Palaeogeography, Palaeoclimatology, Palaeoecology*, 220(3–4), 333–360. <https://doi.org/10.1016/j.palaeo.2005.01.011>
- Youngs, R. R., & Coppersmith, K. J. (1985). Implications of fault slip rates and earthquake recurrence models to probabilistic seismic hazard estimates. *Bulletin of the Seismological Society of America*, 75(4), 939–964. <https://doi.org/10.1785/BSSA0750040939>

References From the Supporting Information

- Ambraseys, N. N. (1962). Data for the investigation of the seismic sea-waves in the Eastern Mediterranean. *Bulletin of the Seismological Society of America*, 52(4), 895–913. <https://doi.org/10.1785/BSSA0520040895>
- Egan, S. S., Buddin, T. S., Kane, S. J., & Williams, G. D. (1997). Three-dimensional modelling and visualisation in structural geology: New techniques for the restoration and balancing of volumes. In *Proceedings of the 1996 Geoscience Information Group conference on geological visualisation. Electronic geology special volume* (Vol. 1, pp. 67–82).
- Kane, S. J., Williams, G. D., Buddin, T. S., Egan, S. S., & Hodgetts, D. (1997). Flexural-slip based restoration in 3D, a new approach. In *1997 AAPG annual convention official program A* (Vol. 58).
- Marchetti, A., Ciaccio, M. G., Nardi, A., Bono, A., Mele, F. M., Margheriti, L., et al. (2016). The Italian Seismic Bulletin: Strategies, revised pickings and locations of the central Italy seismic sequence. *Annals of Geophysics*, 59, Fast Track 5, 1–7. <https://doi.org/10.4401/ag-7169>
- Margheriti, L., Nostro, C., Cocina, O., Castellano, M., Moretti, M., Lauciani, V., et al. (2021). Seismic surveillance and earthquake monitoring in Italy. *Seismological Research Letters*, 92(3), 1659–1671. <https://doi.org/10.1785/0220200380>
- Papadopoulos, G. A., & Imamura, F. (2001). A proposal for a new tsunami intensity scale. In *ITS 2001 proceedings* (Vol. 5, pp. 569–577).
- Tanner, P. W. G. (1989). The flexural-slip mechanism. *Journal of Structural Geology*, 11(6), 635–655. [https://doi.org/10.1016/0191-8141\(89\)90001-1](https://doi.org/10.1016/0191-8141(89)90001-1)